Electroluminescent characteristics of organic light emitting devices by close-spaced sublimation

MI-YOUNG HA, JAE-HOON JUNG, MIN-JAE LEE, DA-YOUNG PARK, SEUNG-JUNG CHOI, MORA VEERA MADHAVA RAO, DAE-GYE MOON*
Department of Materials Engineering, Soonchunhyang University, Shinchang, Asan, Chungnam, 336-745, Republic of Korea

We have demonstrated organic light emitting diodes by using a close spaced sublimation method. Small molecular electron-transporting layers of BAlq and TAZ were investigated for improving device performance by using close-spaced sublimation method. It was found that device with an electron transporting layer of TAZ exhibits a better performance compare to BAlq. The white organic light emitting diodes with an ITO/PVK:Ir(piq)$_3$:FIrpic/TAZ/Li/Al structure is chosen as a device with different doping concentration of FIrpic emission materials. The PVK, Ir(piq)$_3$ and FIrpic organic materials as the host and guest emission materials were spin coated at various concentration of FIrpic ranging from 1wt% to 10 wt%. The maximum luminance and current efficiency were 1037 cd/m^2 and 3.26 cd/A, for white organic light emitting diodes with 10 wt% of FIrpic. The white light, with a Commission Internationale d'Eclairage chromaticity coordinates of (0.38, 0.36), is obtained with an applied voltage of 16V, showing a good white emission color for the 10 wt% of FIrpic device.

1. Introduction

Organic light emitting diodes (OLEDs) are the promising solution for large-area, high resolution flat panel display and lightening sources [1-3]. OLEDs have many advantages including easy processing, robustness and inexpensive compared to inorganic counterparts, and they have emerged as the most important display technology for commercial applications [4-6]. OLED-based displays are integrated in many of today's portable phones due to the visual quality, low profile, and low power consumption. These same attributes have led to recent announcements of OLED television technology as well as OLED-based displays integrated on plastic substrates enabling a new generation of information technologies [7-8]. In particular, the low power consumption of OLED-displays has attracted strong interest for many portable commercial applications [9-12]. In fact, the OLED display is rapidly moving from fundamental research into industrial product, creating many new challenges like lower operation voltage and power consumption, and operating under extreme environmental conditions [13-16]. Recent studies reveal that improvement of charge balance is one of the most effective ways for obtaining highly efficient low-voltage OLEDs because the operation at a relatively high voltages will results in a short lifetime of device performance, and stability. In multilayer device structure, holes in the hole transport layer (HTL) are regarded as being transported too quickly, while electrons in the electron transport layer (ETL) are transported too slowly, and as a result, hole simply pass through without generating excitons with the electrons in the emission layer (EML), which manifests as a low current efficiency[19-20]. To overcome this discordance between the hole and electron motilities and to improve the carrier charge balance, many researches have investigated novel structures such as a metal oxide buffer layer, electron or hole blocking layers, and new high electron mobility materials [17-22].

Recently the development of OLED focuses on enhancing the device efficiency and operating lifetime by multilayer device structure. In the multilayer OLED, electron transport layer plays a vital role which can provide efficient electron transport, reduce the potential barrier between the emission layer and the cathode, and prevent the cathode quenching effect by hole-blocking. Concerning the fabrication of OLED, solution process is low cost and is more competitive than the high cost thermal evaporation. Despite some reports about solution-processed OLED, the dissolution problem between the layers still exists in common solution processed multilayers OLED. Therefore the ETL needs to be deposited by thermal evaporation. In addition, if there is no ETL the device needs low work function or unstable cathode, like Ca, Ba or CsF/Al. That is one of the reasons why the lifetime of OLED is less than that of small molecular OLEDs. The cathode LiF/Al, which is commonly used in small molecular organic light emitting diodes, is known to be more stable than the low work function cathode in solution OLEDs [15-20].

Several research groups have been reported for developing white OLEDs, such as multi-EML structure

doped with different color emitting dopants, use of excimer or exciplex formed by one or two dopants, stacked several OLEDs, and doping of several dopants in a single emitting layers. Among them, single EML structure enables lower operating voltage and color stability because it prevent mismatches of energy levels in multiple EMLs, and therefore, higher power efficiency and color stable WOLEDs could be obtained. There are various methods for highly efficient WOLEDs, in particular, phosphorescent OLEDs are most effective ways to meet the requirements of high efficiency due to their ability to efficiently utilize both singlet and triplet excitons[16-20].

The most widely used polymeric host is poly(9-vinylcarbazole) (PVK). This polymer is largely used for hole transport materials because of its good solubility in common organic solvents and excellent film forming properties. Due to its high glass transition temperature and high triplet energy level, PVK is also extensively regarded as a polymeric host. The non-conjugated characteristics of this polymer lead to a triplet energy level that is nearly identical to that of a single carbazole unit. However, PVK is a unipolar host that transports holes only and PVK based devices usually suffer from high driving voltages due to the imbalanced charge carrier transportation [21-25]. The development of emissive OLEDs is notably hampered by the high hole mobility of PVK that is about 3 orders higher than that of electron mobility, resulting in limited device performance[25,27]. Also, the low lying HOMO energy level of PVK (5.8 eV) mismatches the work function of common anodes and results in difficult hole injection. Using the well-known dopants iridium(III) [bis(4,6-disfluorophenyl)pyridinato-N,C$^{2'}$]-picolinate (FIrpic) and tris[1-phenylisoquinolinato-C2,N]iridium(III) were notably reported, by inserting a thin interlayer of electron transport layers of high triplet energy level between the emissive layer and electron transport layer [26-30].

Close-spaced sublimation (CSS) has been widely used in the growth of thin polycrystalline film CdTe/CdS solar cells due to its simplicity and cost-effectiveness. Temperature of the substrate is one of the most important parameters in the CSS technique. Crystallinity and composition of the deposited films is very much varied by substrate temperature. So the effect of temperatures of substrate is of great importance on the polycrystalline films properties deposited by CSS method. It was first proposed by Nicoll for the hetero-epitaxial growth of GaAs on Ge as a technique based on the close separation between the source materials and the substrate. However there have been few reports about the use of CSS as a means of producing epitaxial films of CdTe[31-32].

In this work, PVK doped [tris(1-phenylisoquinoline)iridium(III)] [Ir(piq)$_3$] and different concentrations of FIrpic solutions prepared and the corresponding thin films were obtained by spin-coating on glass substrates. This system has been previously widely investigated by promising combination for efficient white emission. Several groups have been reported phosphorescent OLEDs using PVK as host polymer[11,30]. We also demonstrated high-performance electrophosphorescent OLED by employing iridium complexes doped in polymer hosts. Here we introduced 3-(4-biphenyl)-4-phenyl-5-tert-butylphenyl-1,2,4-triazole] (TAZ) and [aluminum (III) bis(2-methyl-8-quninolinato)-4-phenylphenolate] (BAlq) as an ETL are prepared by close spaced sublimation method for the first time and investigated the effect of the introduction of the device performance. In CSS method for depositing ETL organic layers of OLEDs, the 2-mm substrate-source distance of our evaporation system was employed to reduce the substrate temperature and the low vacuum pressure during deposition was typically higher than 10^{-3} Torr is used. Since the distance between the sublimation source and target substrate is very close in the CSS process, the consumption of organic materials can be reduced in the fabricating OLEDs. In addition, the CSS process does not required the complicated fabrication system because the low vacuum is required to deposit the functional layers.

2. Experimental

Close space sublimated thin films properties are sensitive to various deposition conditions such as substrate-source temperatures, the source-substrate separation and composition of gases in the deposition chamber. Fig.1 shows the schematic diagram of the CSS growth system designed and developed by our group used in the present study. The CSS system is composed of the low vacuum chamber, low vacuum pump, substrate holder, substrate, sublimation source loader, IR lamp, and quartz window. At first, the organic source substrate is prepared by spin coating of the mixed solution on the bare glass substrate. The mixed solution is fabricated by mixing organic materials in a common solvent such as chlorobenzene. The organic source substrate and the target substrate are loaded to the sublimation source holder and substrate holder, respectively. After that, the organic source substrate is heated by IR lamp through the quartz window. The IR lamp is located outside the low vacuum chamber. The nitrogen gas is used to purge the chamber, thermocouple on the target substrate is used to measure the temperature of the target substrate during the sublimation of organic material.

To constitute of OLED devices by the CSS of organic materials, ITO glass substrate was used as anode. It was cut into small rectangular pieces (7 x 7 cm), cleaned with acetone, methanol, isopropyl alcohol. Each plate was rinsed in deionized water after each step. Finally, the substrates were blown dry with nitrogen gas and then treated by O$_2$ plasma for 3 minutes prior to use. OLED devices fabricated in this work have the following configuration: ITO/PVK:Ir(piq)$_3$/TAZ/LiF/Al   and : ITO/PVK:Ir(piq)$_3$:Firpic/TAZ/LiF/Al.

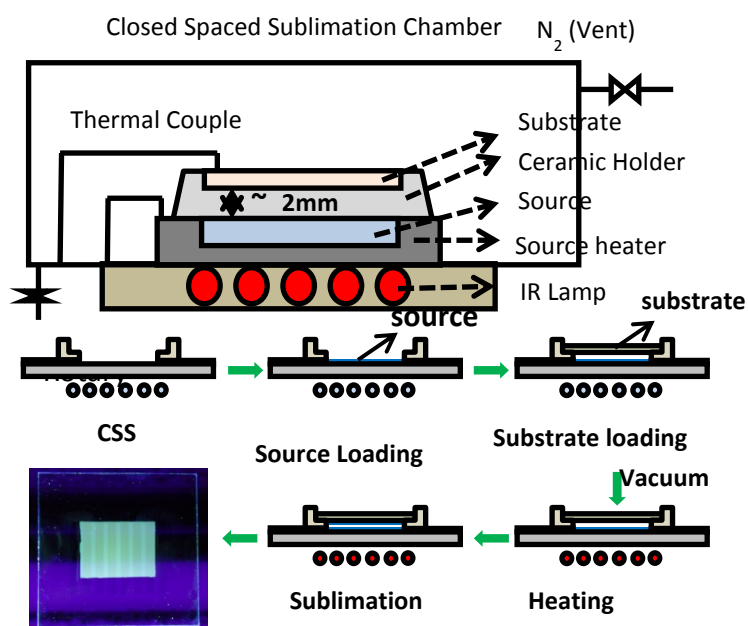Fig.1. Schematic views of the CSS system and process.

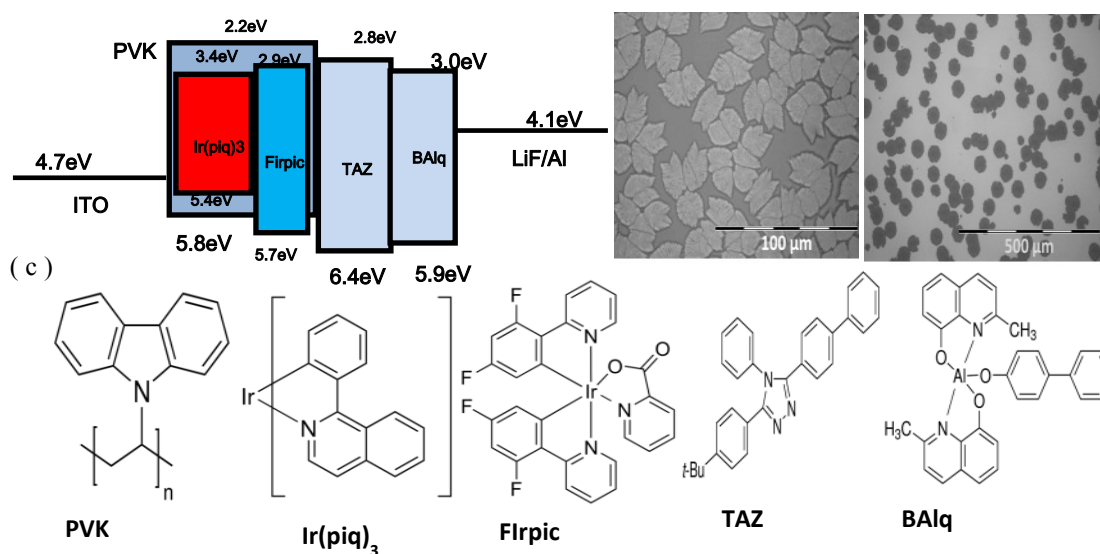(a)   (b)

(c)

Fig.2. (a) Device energy diagrams, (b) microstructures and (c) chemical structures of the organic compounds .

The emissive layer, we blend FIrpic and Ir(piq)$_3$ into PVK with the ratio PVK:Ir(piq)$_3$ (60 nm, 1 wt%), PVK:Ir(piq)$_3$ (1 wt%):FIrpic (1 wt%) (60 nm), PVK:Ir(piq)$_3$ (1 wt%):FIrpic (2 wt%) (60 nm) and PVK:Ir(piq)$_3$ (1 wt%):FIrpic(10 wt%) (60 nm). The emissive layer is then annealed at 80°C for 60 min. After loading the PVK:Ir(piq)$_3$ or PVK:Ir(piq)$_3$:Firpic coated substrates into the CSS chamber, 20 nm thickness of TAZ or BAlq layers was coated by closed spaced sublimation. TAZ layer acts as an electron transporting and hole blocking layer. The cathode was deposited by using

vaccum vapor evaporation. The deposition rate was controlled by a calibrated quartz crystal oscillator and was maintained at 0.1 Å/s for LiF and 2 Å/s for Al. The base pressure in the chamber was about 10^{-6} Torr. A shadow mask was used for the deposition of the cathode. The active area of the devices was 4 x 4 mm.   The photoluminescence (PL), electroluminescence (EL) and current-voltage-luminance characteristics of the devices were obtained by the Keithley 2400 source-meter measurement unit and a Minolta CS 1000 spectro-radiometer.
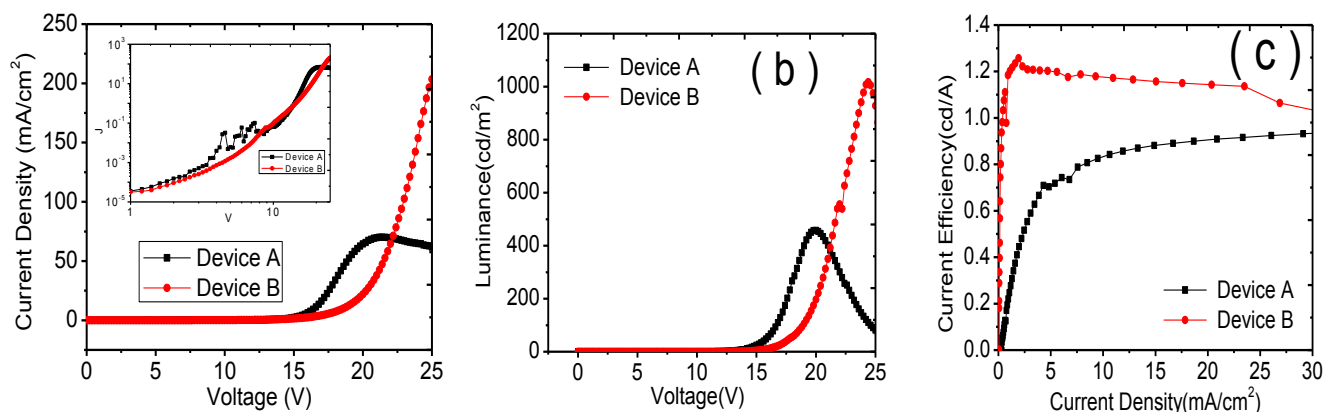
Fig.3. (a) Current density-voltage, (b) luminance- voltage, and (c) current efficiency-current density characteristics of the Device A and Device.

3. Results and discussion

Fig.2(a) illustrates the energy levels diagram of each materials and device structure. Fig.2(b) shows the microscopic images of TAZ, BAlq films that were grown by CSS process at a source temperature of 140 °C,160 °C and a substrate temperature of 42 °C, 48 °C for a growth time of 5 min. It has been reported that the growth temperature and time are important factors to control micro-structures. In our experiments, crystallization was observed that increasing source temperature 160 °C, 180 °C growth time 5 min of TAZ and BAlq films. The chemical structures of all commercially available compounds are shown in Fig.1(c). In OLEDs, $Ir(piq)_3$ and FIrpic are the widely used dopants in PVK. So it is interesting to study the transport properties of PVK films doped with $Ir(piq)_3$ and FIrpic respectively. We look into the highest occupied molecular orbital (HOMO) and lowest unoccupied molecular orbital (LUMO) energy levels of the PVK host, the Ir complexes as shown in Figure 1(a). We note that the HOMO levels of $Ir(piq)_3$ (5.4 eV) and FIrpic (5.7 eV) are lower/higher than that of PVK (5.8 eV)[21-22].   The device structures are as follows:

Device A: ITO/ PVK : $Ir(piq)_3$ (1wt%)[60 nm] / TAZ [20nm] / LiF [0.5nm] / Al [100nm]

Device B: ITO/ PVK : $Ir(piq)_3$ (1wt%)[60 nm] / BAlq [20nm] / LiF [0.5nm] / Al [100nm]

Device C: ITO/ PVK : $Ir(piq)_3$ (1wt%): Firpic (1wt%)[60nm] / TAZ [20nm] / LiF [0.5nm] / Al [100nm]

Device D: ITO/ PVK : $Ir(piq)_3$ (1wt%) : Firpic (2wt%)[60 nm] / TAZ (20nm) / LiF [0.5nm] / Al [100nm]

Device E: ITO/ PVK : $Ir(piq)_3$ (1wt%): Firpic (10wt%)[60nm] / TAZ [20nm]/ LiF [0.5nm) / Al [100nm]

The current density-voltage curves,[log J-log V [in set Fig. 3(a)]], shows two different regimes for the TAZ and BAlq devices. The power-law dependence of current on voltage, $J-V^2$, was observed at low bias and the behavior was attributed to trap-charge limited effects. In this regime, reduced carrier mobility is observed due to the charge capture in traps. As the bias is increased, additional charge is injected, filling a limited number of traps until the trap-filled limit, is reached around 16V, after this empty traps reduction, a rapid increase of effective carrier mobility and a high power law gain in currents, $J-V^8$, are observed, Thus, the device exhibits space-charge limited currents, space charge limited currents[33]. Fig. 3(b) shows the luminance-voltage curves of OLEDs made of two kinds of TAZ and BAlq as the electron transport layer. From those curves, one can easily grasp that TAZ as ETL has much better electron transporting property than that of BAlq. The turn-on voltage was lowered about 2.4V to get a luminance of 200 cd/m^2 by using TAZ layer, from 20V to 17.6V. Fig.3(c) shows the results of OLED devices, two different electron transport layers, current efficiency is clearly improved by Device A compared to Device B. The highest current efficiency of the devices TAZ and BAlq reaches values of 1.2 cd/A and 0.9 cd/A at 20V respectively. Device A with an ETL of TAZ showed higher efficiency than Device B with ETL of BAlq because TAZ (2.8 eV) has higher triplet energy than $Ir(piq)_3$ (2.13 eV). On the other hand, BAlq (2.6 eV) has higher triplet energy than $Ir(piq)_3$ [24-25].
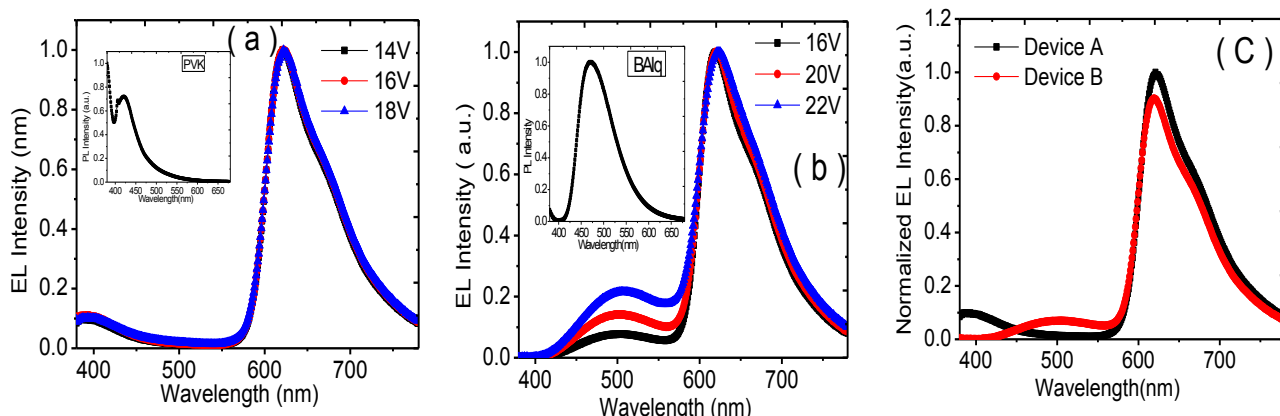
Fig.4. (a) EL spectra of the Device A, (b) EL spectra of the Device B and (c) Normalized EL spectra of the Device A and Device B at 16V.
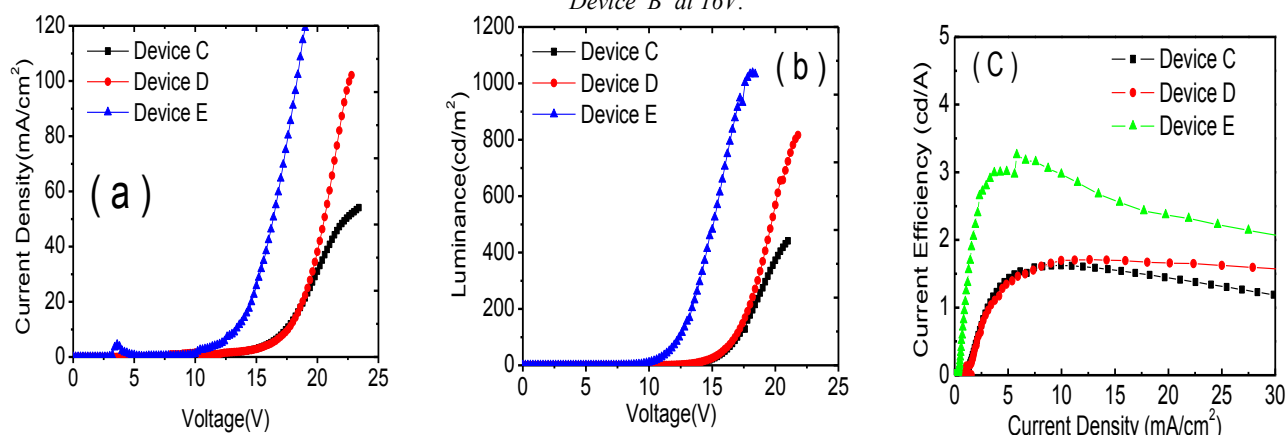

Fig. 5. (a) Current density – voltage, (b) luminescence – voltage and (c) current efficiency-current density characteristics of the Device C, Device D and Device E.
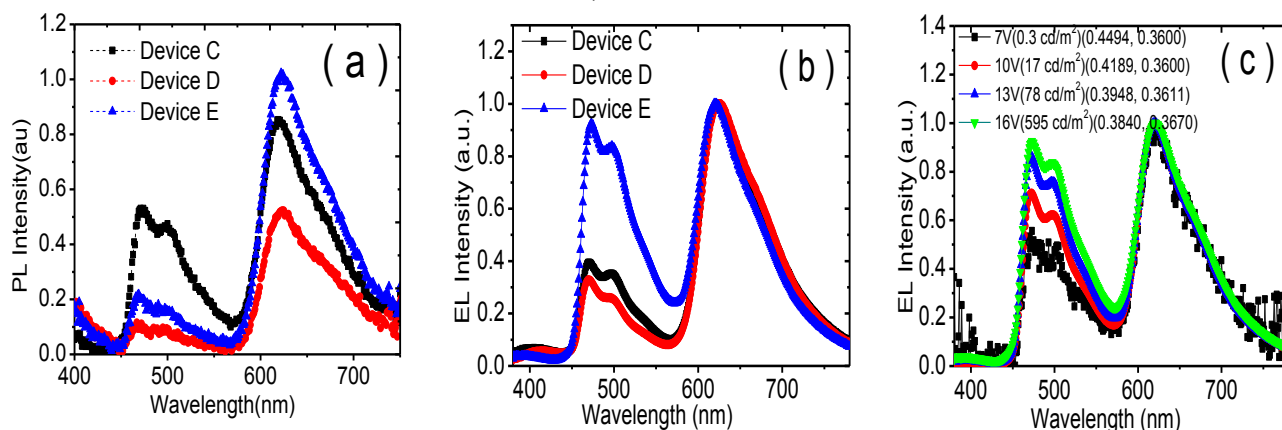

Fig. 6. (a) PL spectra, (b) EL spectra of the Device C, Device D and Device E (c) EL spectra of the Device E at different voltages.

Fig.4(a) and 4(b) shows the EL spectra of the Devices A and Device B at different voltages. In the EL spectra, the emission from the host of PVK with Ir(piq)$_3$ doping concentration. However, Device B, the emission from PVK was observed doping concentration of 1 wt%, indicating incomplete energy transfer from PVK to Ir(piq)$_3$. In contract, Device A the EL emission from PVK was completely quenched at Ir concentration of 1 wt%, indicating that the charge-trapping plays an important role in the operation of the devices. In set fig. 4(a) and 4(b) shows the corresponding PL spectra of the PVK and BAlq layers.

Fig.4(c) shows the normalized EL spectra of the TAZ and BAlq devices at the voltage of 16V. As we can see, the relative red emission of device TAZ to device BAlq decreases sharply. The spectra of TAZ and BAlq devices show mainly red emission peak at 622 and 618 nm originating from Ir(piq)$_3$. In view of this, we can suppose that the motivation of doping Ir(piq)$_3$ into the device is to facilitate the red emission. In devices TAZ and BAlq, relatively decreased red emission of device is mainly due to the reduced electrons concentration in the red emission by the Ir(piq)$_3$ because the good electron transport property. Based on the above, we can conclude that the

variation from devices is mainly due to the higher LUMO level and good electron transport properties of $Ir(piq)_3$ which leads to the distribution of the carriers and the extended recombination zone. The current density-voltage and luminance-voltage characteristics of doping concentration devices namely Device C, Device D and Device E were shown in Fig.5. The turn-on voltage(defined as the voltage when organic device luminance reached 1 cd/m^2) of 1%, 2% and 10% doping concentration devices were 12V, 11.8V and 8.4V respectively. As the forward bias increased, the luminance of organic devices enhanced sharply and reached to the maximum values of 469 cd/m^2(22V), 821 cd/m^2(22V) and 1037 cd/m^2(18.2V) for 1%, 2% and 10% doping concentration devices respectively. The device luminance changing trends of different doping concentration devices were in conformity with the current density, which were the higher doping concentration organic devices showed lower device luminance at the same bias voltage.

The device performance shows a strong dependence on the doping concentration. When the doping concentration is higher, the current density increases apparently at the same voltage. The change in the current density may be explained as follows. At low FIrpic concentration, carrier transport is controlled by the slow release of carrier form FIrpic molecules acting as traps. It then leads to lower current density. However, two effects may arise at higher FIrpic concentration. One possible effect is that, the increase in FIrpic concentration induces the band bending due to the traps and favors charge injection into the host emissive layer[16,30]. The other possible effect is that both dopants and host rather than only the host material participate in transport because the distance between the FIrpic molecules become shorter. Then they both lead to higher current density. Because the change in current density is correlated with the concertation of dopant, the doped FIrpic could be regarded as an efficiency trap for the injected carriers and the charge trapping mechanism should be considered. FIrpic, $Ir(piq)_3$ and PVK of the HOMO levels of 5.6, 5.4, 5.8 eV and LUMO levels of 2.9, 3.4, 2.2 eV, which were indicating that doped materials within in level of host, suggesting this mechanism was reasonable. Due to the existence of barriers at ITO/PVK and PVK/TAZ interfaces, it would cause higher turn-on voltages more than 10V in the devices[34-37].

As shown in Fig.5(c) the current efficiency of devices C-D increased as the concentration of FIrpic increased from 1 wt% to 10 wt%. The maximum luminance is 1037 cd/m^2 and maximum current efficiency is 3.26 cd/A. Unfortunately our results not so far good, the reason for Ir complexes red dye is the deepest hole trap in the PVK host and trapped holes will attract electrons and facilitate electron injection from the cathode. It is probably because the triplet energy of PVK is not high enough to confine the triplet excitons of blue Ir complexes (FIrpic). Indeed the host used for blue FIrpic OLED is much higher than PVK. Such superior host for OLED seems yet to be discovered. Li et al. reported a white light from a single emitting component device with a maximum brightness of 1200

cd/m^2 at 18V and current efficiency of 1.1 cd/A[38], similar device by Liu et al., disclosed the maximum brightness was 1395 cd/m^2 and current efficiency was 2.07 cd/A at the drive voltage of 16V[39], and another device by Rao et al. obtained from multiple-emissive-layer structure of white emission with maximum current efficiency of 1.93 cd/A[40].

The normalized photo-luminance (PL) spectra of PVK:$Ir(piq)_3$ thin films doped with FIrpic at different weight ratios: 1%, 2% and 10%. The PL spectrum of devices are shown in Fig.6(a). PL peaks are observed at 410 nm for PVK singlet emission. Below a critical FIrpic concentrations of 10wt%, the Forster transfer of excitons is incomplete because of the large average separation between an excited site on the PVK and $Ir(piq)_3$. Therefore an emission near 410nm attributed to the PVK host is observed. The separation reduces the exciton transfer efficiency and improves with increasing concentration of FIrpic, leading to almost complete disappearance of the emission near 410 nm at FIrpic concentrations. In the spectra of the blended thin films, the peaks at 410 nm, 475 nm and 620 nm originated from PVK, FIrpic and $Ir(piq)_3$ emission was observed. This is to say that, FIrpic and $Ir(piq)_3$ was not completely quenched even at high concentration. Since the triplet energy level of PVK (2.5 eV) is lower than that of FIrpic (2.62 eV) and higher than that of $Ir(piq)_3$ (2.13 eV) energy back transfer occurs from the triplet excitons the FIrpic to the low-lying triplet states of PVK that causes the FIrpic quenching. Therefore, in the PL process, FIrpic was quenched by PVK because of the low-lying triplet energy level of PVK. The EL spectra depicted in Fig.6 (b) indicate that the FIrpic and Ir(piq)3 energy transfer becomes efficient in the present device. The spectra cover all wavelengths from 450 to 750 nm, the applied voltage changes from 10V to 16 V, the CIE coordinates vary slightly from (0.42, 0.36) to (0.38, 0.36). Thus, a high performance WOLED has been achieved by optimizing the device structure [33-36].

Figure 6 (c) displays the EL spectra of Device E at different voltages, where the EL intensity is normalized to the maximum wavelength peak. Clearly, the emission from FIrpic increases with the increase in driven voltages, which should be related to the different role of PVK, $Ir(piq)_3$ and FIrpic molecules in the trapping and transport in EL processes. As we can see that device shows poor color stability in spectra that the blue emission increases sharply with the increasing voltage, mainly due to the voltage induced exciton recombination zone alteration. However, our device show good color stability CIE coordinates shift of (0.035, 0.007) with a voltage from 10 to 16V. However, in EL spectra of all devices, unexpected peaks shift in range about 390 to 410 nm, which considered emission came from the exciplex formed at the interface between the emissive layer and the ETL due to over-populated hole carriers in the emissive layers. Particularly, compared to the other devices 1 wt%, 2wt%, and device 10 wt% showed the most significant peak shift in range about 390 nm to 410 nm and thus EL of device 10wt% showed the color impurity. White OLED needs more work to solve the reproducibility of red and blue

OLEDs efficiency. Furthermore the stability of the device is not good compared with fluorescent solution based OLED. In fact this is general problem for OLED with PVK host doped with Ir complexes.

4. Conclusions

1. We have successfully deposited electron transport layers (TAZ and BAlq) by using a close spaced sublimation process.

2. The organic material consumption of the CSS process was very small. Single emissive layer devices with white light emission consisting of the two phosphorescent emitters Ir(piq)$_3$, FIrpic and PVK polymer host components.

3. Using optimized phosphorescent dopant concentration of FIrpic and Ir(piq)$_3$ in the PVK host of the single emissive layer, white OLED showed a maximum luminance of 1037 cd/m^2, and current efficiency of 3.26 cd/A at 16V, with CIE color coordinates of (0.38, 0.36).

4. Consequently triplet excitons were not properly transferred from host to dopant and dopant to dopant generating a not well balanced emission with energy loss through optimizing the concentration of the two phosphorescent dopants in a single emissive layer of white PLED devices.

Acknowledgements

References

[1] C.W. Tang, S. A. VanSlyke, Appl Phys Lett, **51**, 913 (1987).
[2] Y. Sun, N.C. Giebink, H. Kanno, B. Ma, M.E. Thompson, S.R. Forrest, Nature, **440**, 908 (2006).
[3] S. J. Su, E. Gonmori, H. Sasabe, J. Kido, Adv. Mater., **20**, 4189 (2008).
[4] S. Reineke, F.Lindner, G. Schwartz, N. Seidler, K. Walzer, B. Lussem, K. Leo, Nature, **459**, 234 (2009).
[5] B.W. D'Andrade, S.R. Forrest, Adv. Mater., **16**, 1585 (2004).
[6] Y. Sun, S.R. Forrest, Org. Electron., **9**, 994 (2008).
[7] L. Ying, C.L. Ho, H.B. Wu, Y. Cao, W.-Y. Wong, Adv. Mater., **26**, 2459 (2014).
[8] X. Guo, C.J. Qin, Y.X. Cheng, Z.Y. Xie, Y.H. Geng, X.B. Jing, F.S. Wang, L.X. Wang, Adv. Mater, **21**, 3682 (2009).
[9] Szuheng Ho, Shuyi Liu, Ying Chen, and Franky So, J. of Photonics for Energy, **5**, 057611 (2015).
[10] H. Sasabe, J. Kido, J. Mater. Chem. C., **1**, 1699 (2013).
[11] S. Reineke, M. Thomschke, B. Lussem, K. Leo, Rev. of Modern Phys., **85**, 1245 (2013).
[12] N. Sun, Y. Zhao. Y. Chen, D. Yang, J. Chen, D. Ma, Appl. Phys. Lett., **105**, 013303 (2014).
[13] F. Zhano, Z. Zhang, Y. Liu, Y. Dai, J. Chen, D. Ma, Org. Electron., **13**, 1049 (2012).
[14] G. T. Lei, L. D. Wang, L. Duan, J. H. Wang, Y. Qiu, Synth. Met., **144**, 249 (2004).
[15] Y.S. Park, J.W. Kang, D.M. Kang, J. W. Park, Y.H. Kim, S.K. Kwon, J. J. Kim, Adv. Mater., **20**, 1957 (2008).
[16] Q. Wang, D. Ma, Chem. Soc. Rev., **39**, 2387 (2010).
[17] C. Weocjse, S.Reoneke, M. Furno, B. Lussem, K. Leo, J. Appl. Phys., **111**, 033102 (2012).
[18] J. Wang, F. Zhang, W. Tang, A. Tang, H. Peng, Z. Xu, F. Teng, Y.Wang, J. of Photochem and Photobio. C: Photochem. Rev., **17**, 69 (2013).
[19] X. Xu, G. Yu, Y. Liu, D. Zhu, Displays, **27**, 24 (2006).
[20] C. Zhong, C. Duan, F. Huang, H. Wu, Y. Cao, Chem. Mater., **23**, 326 (2011).
[21] Kang-Hee Kim, Yu-Seok Seo, Dae-Gyu Moon, Synth. Metals, **189**, 157 (2014).
[22] Yu-Seok Seo, Dae-Gyu Moon, Current Appl. Phys., **14**, 1188 (2014).
[23] Jae-Hoon Jung, Dae-Gyu Moon, Mol. Cryst. and Liq. Crysta., **601**, 215 (2014).
[24] S. Yasuhiko, K. Hiroshi,Chem. Rev., **107**, 953 (2007).
[25] N. Thejokalyani, S.J. Dhoble, Renewable and Sustain. Energy Rev., **32**, 448 (2014).
[26] P. Chen, L. Zhao, Y.Duan, Y. Zhao, W.F. Xie, G.H. Xie, S.Y. Liu, L.Y. Zhang, B. Li, J. of Luminance., **131**, 2144 (2011).
[27] J. Pina, J. Seixas de Melo, H. D. Burrows, A. P. Monkman, and S. Navaratnam, Chem. Phys. Lett., **400**, 441 (2004).
[28] J. Chen, F. Zhao, D. Ma, Mater. Today, **17**, 175 (2014).
[29] J.H. Seo, S.J. Le, B.M. Seo, S.J. Moon, K.H. Lee, J.K. Park, S.S.Yoon, Y.K. Kim, Org. Electron., **11**, 1759 (2010).
[30] T.H. Kim, H.K. Lee, O.O. Park, B.D. Chin, S.H. Lee, J.K. Kim, Adv. Funct. Mater., **16**, 611 (2006).
[31] N. Romeo, A. Bosio, V. Canevari, A. Podesta, Solar Energy, **77**, 795 (2004).
[32] F.H. Nicoll, J. Electrochem. Soc., **110**, 1165 (1963).
[33] L.S. Hung, C.H. Chen, Materials Science and Engineering R., **39**, 143 (2002).
[34] Q. Wang , J. Q. Ding , D. G. Ma , Y. X. Cheng , L. X. Wang , F. S. Wang , Adv. Mater., **21**, 2397 (2009).
[35] S. H. Eom , Y. Zheng , E. Wrzesniewski , J. Lee , N. Chopra, F. So, J. Xue , Appl. Phys. Lett., **94**, 153303 (2009).
[36] S. Chen, H.S. Kwok, Org. Electron., **13**, 31 (2012).
[37] J. Lee, J.I. Lee, H.Y. Chu, Synth. Metal., **159**, 991 (2009).
[38] J. Y. Li, D. Liu, C. Ma, O.Lengyel, C.S.Lee, C.H.Tung, S.T. Lee, Adv. Mater., **16**, 1538 (2006).
[39] Y. Liu, M. Nishiura, Y. Wang, Z. Hou, J. Am. Chem. Soc., **128**, 5592 (2006).
[40] M.V.M. Rao, Y.K.Su, T.S.Huang, Y.C.Chen, Nano-Micro Lett., **2**, 242 (2010).

*Corresponding author: dgmoon@sch.ac.kr